Biomaterials Science

Multi-stage, charge conversional, stimuli-responsive nanogels for therapeutic protein delivery

Journal:	*Biomaterials Science*
Manuscript ID:	BM-ART-06-2015-000171.R1
Article Type:	Paper
Date Submitted by the Author:	16-Jul-2015
Complete List of Authors:	Zhang, Xuejiao; Freie Universität Berlin, Institut für Chemie und Biochemie, Zhang, Kai; Charité-Universitätsmedizin Berlin, Institut für Laboratoriumsmedizin, Haag, Rainer; Freie Universit�t Berlin, Institut f�r Chemie / Organische Chemie

Multi-stage, charge conversional, stimuli-responsive nanogels for therapeutic protein delivery

Xuejiao Zhang[1,*], Kai Zhang[2], Rainer Haag[1]
1 Freie Universität Berlin, Institut für Chemie und Biochemie, Takustraße 3, 14195 Berlin, Germany
2 Charité-Universitätsmedizin Berlin, Institut für Laboratoriumsmedizin, Klinische Chemie und Pathobiochemie, 13353 Berlin, Germany

Corresponding author:
Xuejiao Zhang
Institute for Chemistry and Biochemistry
Freie Universität Berlin
Takustrasse 3, Berlin 14195 (Germany)
E-mail: zhangxuejiao1985@gmail.com

ABSTRACT

A boronate ester crosslinked zwitterionic nanogel (NGCA) with ATP/pH-sensitivity has been developed with an inverse nanoprecipitation technique to achieve a two-stage charge conversion that responds to tumor extracellular conditions (pH 6.5-6.8) and an intracellular acidic environment (pH 5-6). Cationic cytochrome C (CC), a therapeutic protein, has been encapsulated into NGCA through inverse nanoprecipitation via electrostatic interaction, to form protein-loaded nanogel (NGCA-CC). By adjusting the ratio of the amino and carboxyl groups in the nanogels, negatively charged nanogels that are safer under physiological conditions (pH 7.4) can convert their surface charge to positive at tumor extracellular pH, which enhance their cellular uptake efficiency. The citraconic amide formed from citraconic anhydride and amine can be cleaved in the intracellular acidic organelles to expose more amino groups and facilitate endosomal escape. The release of CC is accelerated in the presence of 5 mM ATP or under acidic conditions. Confocal laser scanning microscopy (CLSM) and flow cytometry have shown that NGCA-CC's cell uptake is higher at pH 6.5 than 7.4. MTT and real-time cell analysis (RTCA) have illustrated that there is more toxicity at pH 6.5 than at pH 7.4. The apoptosis process induced by CC was determined by flow cytometry.

Keywords: polyglycerol nanogel, charge conversion, protein delivery, nanogel degradation, cellular uptake

1. Introduction

Since the first FDA approved recombinant protein therapeutic human insulin entered the market in 1982, protein therapeutics have played a vital role for the treatment of various diseases, because of their high specificity, limited side effects, and predominant anticancer efficacy.[1-3] Various carrier systems have been developed to surmount the obstacles of protein therapeutics, such as instability, poor bioavailability, and low cell internalization efficiency.[4-7]

The surface charge exerts a great impact on the safety and stability of nanocarriers during blood circulation. Positively charged nanoparticles possess higher affinity with the negatively charged cell membrane, which facilitates cellular uptake, whereas their severe cytotoxicity, strong interactions with blood components, and rapid clearance often impede the in vivo applications.[8-10] Development of pH-induced charge conversional drug delivery systems can help to overcome the intrinsic pH difference between tumor tissues (pH 6.5-6.8) and normal tissues or blood stream (pH 7.2-7.4).[11-15]

Reactions of 2,3-dimethylmaleic anhydride (DMMA) and amino groups on the particle surface have been used to shield the positive charge of nanoparticles.[16-18] The generated amide bond is cleavable under mildly acidic conditions but stable at neutral or basic pH,[19] whereas the DMMA-decorated nanoparticles are inert under physiological conditions. After accumulating in the acidic tumor tissue through the enhanced permeation and retention (EPR) effect, the amide bond slowly cleaves and thus exposes the positive charge which eventually promotes cell internalization.[20] However, the cleavage of the amide bond is not prompt so that the charge conversion is delayed. Furthermore, the amide bond can also be slowly cleaved at neutral pH, but this is not propitious for long-term in vivo circulation.[21]

Zwitterionic nanoparticles with both anionic and cationic surface moieties, on the other hand, can rapidly change their surface charge at their isoelectric pH.[22, 23] By adjusting the ratio of anionic and cationic components, instantaneous charge conversion from negative to positive can be achieved under tumor extracellular pH, which enhances internalization efficiency.

Another challenge for protein delivery is the acidic environment of cellular organelles. After endocytosis, the pH drops to 5-6 in the endosome/lysosome, where both the nanoparticles and their protein payloads can be degraded by endolysosomal acid and hydrolyase.[22] Therefore, it is necessary for the nanocarriers to liberate their encapsulated proteins into the cytoplasm through endosomal escape. Kataoka et al. have reported that citraconic amide, formed from citraconic anhydride and primary amines, cleaved at endosomal pH and induced the release of primary amines that promoted the endosomal escape of the protein into cytoplasm by disrupting the endosomal membrane.[12, 24, 25]

We here present a zwitterionic nanogel with two-stage charge conversional properties that we designed to respond to slightly acidic tumor extracellular conditions (pH 6.5-6.8) and an intracellular acidic environment (pH 5-6). As shown in Figure 1, the negatively charged zwitterionic nanogels become positive once accumulating into slightly acidic tumor tissue, which favors their endocytosis. Hydrolysis of citraconic amide in the acidic intracellular organelles (endo/lysosome) exposes more amine groups and results in the second-stage charge conversion. The more elevated positive charge presumably interrupts the endo/lysosome membrane and facilitates endosomal escape. The high concentration of ATP made the nanogels degrade in the cytosol, which induced the protein release.

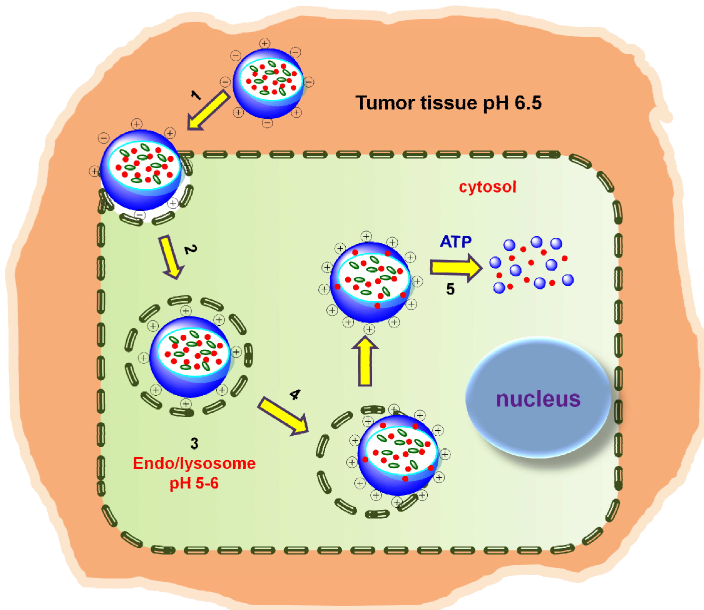

Figure 1. Schematic illustration of a two-stage charge conversion process of zwitterionic nanogels. (1) First stage charge conversion: from negative to positive owing to the decreased pH in tumor tissue compared to blood circulation, (2) cellular uptake by endocytosis, (3) second stage charge conversion: elevated positive charge due to the hydrolysis of citraconic amide, (4) endosomal escape, (5) dissociation of nanogels and drug release triggered by ATP in the cytosol.

2. Materials and Methods

2.1. Materials

Dendritic polyglycerol (dPG, M_n = 5.8 kDa, M_w = 7.5 kDa, PDI = 1.29) was synthesized based on the published procedure.[26, 27] 2-formylphenylboronic acid (FPBA), fluorescein isothiocyanate (FITC), and cytochrome C (CC) were purchased from Sigma-Aldrich (Germany). 4'6-diamidino-2-phenylindole (DAPI), FM® 4-64 Dye (*N*-(3-Triethylammoniumpropyl)-4-(6-(4-(diethylamino) phenyl) hexatrienyl) pyridinium dibromide), and Dead Cell Apoptosis Kit with Annexin V Alexa Fluor® 488 & propidium iodide (PI) were purchased from Lifetechnology (Germany). All other chemicals were purchased from Aldrich (Germany) or Acros (Germany). For cell culture experiments, MCF-7 cells (DSMZ no.: ACC 115) cultured in RPMI supplemented with 10% fetal calf serum, MEM nonessential amino acids, 1 mM sodium pyruvate, and 10 µg/ml human insulin in a humidified atmosphere (5% CO_2) were used.

2.2. Characterization

^1H NMR spectra were recorded on a Bruker ECX 400. The residual deuterated solvent peaks were used as internal standard to calibrate the chemical shifts. The size and zeta potential were determined by a Zetasizer Nano-ZS from Malvern Instruments equipped with a 633 nm He-Ne laser at 25 ^oC. The UV measurements of CC and FITC-CC were carried out at 408 and 495 nm, respectively. Circular dichroism (CD) spectra were recorded on a Jasco J-715 spectropolarimeter at 20 ^oC (Jasco PTC-348 WI peltier thermostat).

2.3. Synthesis of dPGA-FPBA

dPG with 90% amine functionalities (dPGA) was synthesized by a published three-step procedure.[28, 29] FPBA (151.8 mg, 1.01 mM) and dPGA (1 g, 0.175 mM) were dissolved in 20 ml methanol in a round-bottom flask and the mixture was stirred overnight under argon atmosphere, which was followed by the addition of three equivalents $NaBH_4$ (114.5 mg, 3.03 mM) to reduce the imine bond. The pure product (FPBA functionality 5%, conversion 75.1%, yield 72.5%) was obtained by lyophilization after extensive dialyzing against distilled water (molecular weight cut-off 2000 Da). ^1H NMR (400 MHz, D_2O, 25 ^oC): δ = 2.48-3.18 (-CH_2-NH_2 or –CH-NH_2), 3.33-4.18 (dPG backbone), 7.11-7.53 (4H, ArH).[30]

2.4. Synthesis of dPGA-FPBA-CA

dPGA-FPBA (500 mg, 5.74 mmol of primary amine) was dissolved in pyridine (10 ml) and a certain amount of citraconic anhydride (CA) was added dropwise into the solution. The reaction was stirred overnight at room temperature, and then 1 M $NaHCO_3$ solution (50 ml) was poured into the solution. The compound was purified with Amicon Ultra filter (3 kDa MWCO, Millipore) by centrifuging it 4 times in $NaHCO_3$ solution and 3 times in distilled water. The pure conjugate with respectively 35%, 50%, and 65% CA functionalities was yellow powder after lyophilization. ^1H NMR (400 MHz, D_2O, 25 ^oC): δ = 5.51-5.90 (1H, CO*CH*CH_3COONa), 1.88-2.04 (3H, COCHCCH_3COONa).

2.5. Synthesis of nanogel (NGCA) by inverse nanoprecipitation

10 mg of dPGA-FPBA-CA was dissolved in 1 ml Milli-Q-water and 4 ml of dPG (10 mg/ml) aqueous solution was added. The mixture was injected into 200 ml acetone in a 500 ml round-bottom flask under intensive stirring, forming turbid solution. As soon as the mixture was homogeneous, the stirring was stopped and the in situ gelation was performed overnight at room temperature. The NGCA was purified by evaporating acetone and then ultrafiltrating with Amicon Ultra filter (10 kDa MWCO, Millipore) 4 times in Milli-Q-water. After lyophilization, the pure NGCA was obtained.

2.6. Preparation of CC-loaded nanogel (NGCA-CC)

20 mg of CC was added to 5 ml aqueous solution containing 10 mg dPGA-FPBA-CA with different CA functional percentages and 40 mg dPG. The mixture was immediately injected into 200 ml acetone with intensive stirring, followed by 24 h

immobilization. Acetone was evaporated and the residue was ultrafiltrated with Amicon Ultra filter (100 kDa MWCO, Millipore) 5 times in Milli-Q-water in order to remove the free CC. NG-65%CA-CC, NG-50%CA-CC, and NG-35%CA-CC were obtained by lyophilization and the loading capacity of CC was examined by UV-vis at 408 nm.[31] FITC-labeled CC (CC-FITC) was loaded into the nanogel following the same procedure.

2.7. pH-induced charge conversion and citraconic amide hydrolysis

To explore the pH-induced first-stage charge conversion of the zwitterionic nanogel, the zeta potential was measured at different pH values in the process of pH titration. 16 mg NGCA-CC with different percentages of CA moieties was respectively dispersed in 8 ml of PBS solution at pH 10.5 adjusted by NaOH solution. 0.1 and 0.01 M HCl solutions were used to titrate the substances, and the zeta potentials were measured at various pH values by a Zetasizer Nano-ZS (Malvern, UK).

To examine the hydrolysis of citraconic amide at different pH values, 10 mg NGCA was suspended in 10 ml of PBS at pH 7.4 or acetate buffer at pH 5 at 37 ^{o}C. At different time intervals, 1 ml of each nanogel suspension was subjected to the zeta potential measurement by a Zetasizer Nano-ZS (Malvern, UK).

2.8. ATP/pH-triggered degradation of NGCA

10 mg NGCA was homogeneously suspended in 10 ml different buffer solutions and incubated in a water bath at 37 ^{o}C under continuous stirring. The size changes over time were measured by DLS.

2.9. Protein release study

1 ml of NGCA-CC suspension (10 mg/ml) in PBS solution (pH 7.4) was transferred to a dialysis tube (molecular weight cut-off 300 kDa) and immersed into 30 ml of different release medium solutions at 37 ^{o}C with continuous stirring (200 rpm). At predetermined time intervals, 5 ml of release medium was taken out and replenished with an equal amount of fresh medium. The absorbance of CC was detected by UV-vis spectrophotometer at 408 nm for quantification. The release experiments were performed in triplicate, and the results represented a mean value with standard deviations. The released CC was collected and lyophilized. CD spectroscopy was conducted to measure the conformational change of the released CC compared to the free CC at a concentration of 0.5 mg/ml over the wavelength range from 190 to 240 nm.

2.10. Cytotoxicity

All cell culture experiments were performed in accordance with the German genetic engineering law and German biosafety guidelines in an approved biosafety level 1 laboratory.

The MTT assay was used to evaluate the cell toxicity. MCF-7 cells were seeded into 96-well plates at 5000 cells per well and incubated for 24 h. Afterwards, the cell culture medium was removed and replaced with 100 µl supplemented RPMI containing NGCA, NGCA-CC, and free CC at pre-determined concentrations. After 48 h incubation, 10 μl of MTT solution (5 mg/ml in PBS) was added into each well and the cells were further incubated for 2 h. Then the culture medium was completely removed and 100 μl of DMSO was added to dissolve the purple formazan crystals. The absorbance was determined by a microplate reader at the wavelength of 570 nm. The untreated cells were used as a control and the results were reported as the mean value of triplicate experiments with standard deviations.

The effect of pH on the cell proliferation inhibition of NGCA-CC was evaluated by MCF-7 cells with the similar procedure to the above. In brief, MCF-7 cells were seeded in 96-well plates (5000 cells/well). After 24 h incubation, the culture medium was replaced with 100 μl supplemented RPMI at pH 7.4 or 6.5 respectively containing NGCA-CC and CC at the CC concentration of 150 and 200 μg/ml. The cells were incubated for 1 h, and then the medium was replaced by 100 μl of fresh medium at neutral pH. MTT assay was generated after further incubation for 47 h.

2.11. Real-time cell analysis (RTCA)

The RTCA assay was conducted to dynamically monitor the cell proliferation and viability based on the Real-Time Cell Electronic Sensor (RT-CES) system. The cells were cultured in the microelectrode-coupled microtiter plates and the electrode impedance reflected the cell number, cell morphology, and the degree of cell adhesion.[32-35] The cells without treatment attached to the bottom of the well and enhanced the impedance, thereby inducing the increased cell index (CI) value. 50 μl of supplemented RPMI was added to each well of the E-plate (Roche, Mannheim, Germany) for background measurements. Then MCF-7 cells were added into the sensor wells at a concentration of 5000 cells per well for 24 h incubation, followed by replacing the culture medium with NGCA-CC and CC containing fresh medium at different concentrations. The E-plate was incubated for 48 h and monitored on the RTCA SP system (Roche, Mannheim, Germany) with time intervals of 15 min. The RTCA software version 2.0 was used for analysis. The cell proliferation inhibited by NGCA-CC at different pH values was monitored by RTCA device with the similar procedure as discussed in Section 2.9.

2.12. Cellular uptake

MCF-7 cells were seeded at the concentration of 1×10^5 cells per well in a 24-well plate with coverslips on the bottom of the wells. After 24 h incubation, the medium was replaced with fresh cell culture medium containing FM 4-64 (10 μg/ml) and CC or NGCA-CC, where CC was labeled with FITC, at a final CC concentration of 50 μg/ml. Additional 4 h and 24 h incubation was performed before removing the medium and rinsing trice with PBS solution. After being fixed with 4% paraformaldehyde PBS solution for 20 min, the cell nuclei were stained with DAPI for 30 min, followed by dryness. To investigate the effect of pH on the cellular uptake of NGCA, the cells were incubated in the CC or NGCA-CC containing culture medium with FM 4-64 (10 μg/ml) at pH 7.4 or 6.5, respectively. After 1 h, the cells were rinsed with PBS solution, which was followed by fixation and staining. The coverslips were pasted on the microscope slides and examined with a CLSM (Leica, Germany).

Flow cytometry was performed to quantify the cellular uptake. MCF-7 cells were cultured in a 24-well plate at the density of 1×10^5 cells per well for 24 h. Then the medium was removed and replenished with substance-containing fresh medium at pH 7.4 and 6.5. After 1 h, the cells were washed trice with PBS solution after removing the culture medium, followed by harvesting with trypsin. The cells were fixed by 4% paraformaldehyde solution and resuspended in PBS supplemented with 1% fetal calf serum and 0.1% sodium azide. The fluorescence was quantitatively measured by a FACScalibur (Becton Dickinson, Heidelberg, Germany).

2.13. Cell apoptosis

The cell apoptosis induced by NGCA-CC and free CC was evaluated with a Dead Cell Apoptosis Kit (Lifetechnology, Germany). MCF-7 cells were cultured in a 24-well plate at a concentration of 1×10^5 cells per well for 24 h, and then treated with NGCA, free CC, and NGCA-CC, respectively. After a certain time point, the cells were harvested and washed with cold PBS twice, followed by suspension in 100 µl of binding buffer. 5 µl of Annexin V-Alexa Fluor®488 and 1 µl of PI (100 µg/ml) solutions were respectively added into the cell suspensions for 15 min incubation at room temperature under dark conditions. Then 300 µl of binding buffer was added and the cells were immediately analyzed with a FACScalibur (Becton Dickinson, Heidelberg, Germany). A 20 mW blue laser emitting at 488 nm served as the excitation source for Annexin V-Alexa Fluor®488 (FL1) and PI (FL2). Annexin V (green) and PI (red) fluorescent signals were collected at 530 nm and 610 nm pass filters, respectively, for 1×10^4 cells.

3. Results and discussion

3.1. Preparation of NGCA and NGCA-CC by inverse nanoprecipitaion

Scheme 1 shows the fabrication of NGCA and NGCA-CC. dPG was converted to 90% functionalized dPGA according to a three-step procedure published previously.[28, 29] Then FPBA was conjugated with amine groups by a Schiff-base reaction, followed by the reduction with $NaBH_4$. The dPGA-FPBA conjugate was obtained with the secondary amino groups in the ortho position of a phenyl ring. The dative boron-nitrogen interaction (red arrow in Scheme 1) can improve the stability of the boronate ester under physiological conditions.[29] Afterwards, citraconic anhydride (CA) was coupled with some of the remaining amines in dPGA-FPBA to form an amide bond that is stable under neutral or basic conditions, but cleavable at acidic pH. dPGA-FPBA-CA with 35%, 50%, and 65% CA functionalities, respectively, were obtained as macromolecular crosslinkers.

The charge conversional nanogels were generated by using dPG as the main scaffold and dPGA-FPBA-CA as the crosslinker via a surfactant-free inverse nanoprecipitation method.[29, 36, 37] As shown in Scheme 1, the crosslinking occurred through the complexation of 1,2-diols in dPG and boronic acids in dPGA-FPBA-CA. The zwitterionic nanogels (NGCA) were formed with both positively charged amino groups and negatively charged carboxyl groups.

The therapeutic protein, cytochrome C (CC), was co-precipitated with the macromolecular precursors and encapsulated into the nanogels via an electrostatic interaction between the cationic protein and anionic carboxyl groups in the nanogels. The loading capacity of CC was determined by UV-vis as 6.5%, 21%, and 25% for NG-35%CA-CC, NG-50%CA-CC, and NG-65%CA-CC, respectively.

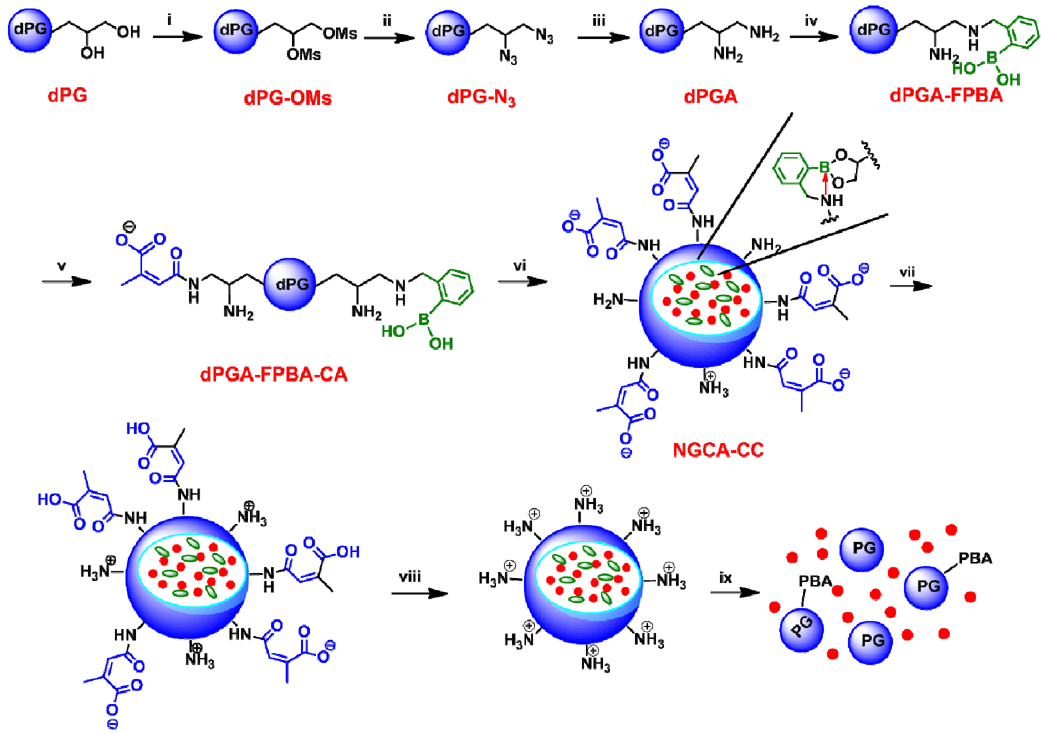

Scheme 1. Synthetic pathway of NGCA-CC: (i) Methanesulfonyl chloride (MsCl), pyridine, 0 °C to r.t., 16 h, (ii) NaN_3, 65 °C, 3 d, (iii) Triphenylphosphine (PPh_3), THF/H_2O, 24 h, (iv) FPBA, methanol/$NaBH_4$, (v) citraconic anhydride, pyridine, r.t., (vi) dPG, CC, inverse nanoprecipitation, (vii) pH 6.5, (viii) pH 5, (ix) ATP.

3.2. pH-induced two-stage charge conversion

To demonstrate the charge conversional properties of the zwitterionic NGCA-CC according to the environmental pH, the zeta potential of NGCA-CC with different CA loadings was measured at various pH values by titration. As shown in Figure 2A, the zeta potentials of all the nanogels were negative at the starting pH of 10.5 and became gradually positive over titration with HCl solution due to the protonation of amino and carboxyl groups. The isoelectric points were 8.5, 7, and 5.8 for NG-35%CA-CC, NG-50%CA-CC, and NG-65%CA-CC, respectively. At tumor extracellular pH (6.5-6.8),[38] NG-50%CA-CC was capable of charge conversion and presented a slightly positive charge, which could promote the tumor cellular uptake. Therefore, all the following experiments were performed with NG-50%CA-CC (abbreviated as NGCA-CC).

Other than the zwitterionic conversion induced by protonation/deprotonation, the

hydrolysis of citraconic amide at endosomal/lysosomal pH (5-6)[39] can cause the second stage charge conversion that is favorable for endosomal escape. Since CC cannot be stably retained inside the nanogel at pH 5 under 37 °C (see Section 3.4), NGCA without CC entrapment was used to perform the hydrolysis study. As shown in Figure 2B, NGCA remained negatively charged during the whole period of measurement at pH 7.4, which is attributed to the relative higher stability of citraconic amide at neutral condition. At pH 5.0, NGCA had an initial negative surface charge of about –5 mV, whereas it reversed to positive within 2 h and continuously increased to the zeta potential of more than +20 mV. This was ascribed to the cleavage of citraconic amide bond, resulting in the exposure of amine groups, which was also proven by the ^{1}H NMR (Figure S1) and ninhydrin reaction (Figure S2).
As illustrated in Figure 2C, NGCA-CC is negatively charged at blood pH (7.4), but becomes positive under tumor tissue pH (6.5), facilitating cellular uptake. After internalization into the tumor cells, the positive charge of NGCA-CC is further increased in the endosome (pH 5) induced by the cleavage of citraconic amide, which promotes endosomal escape.

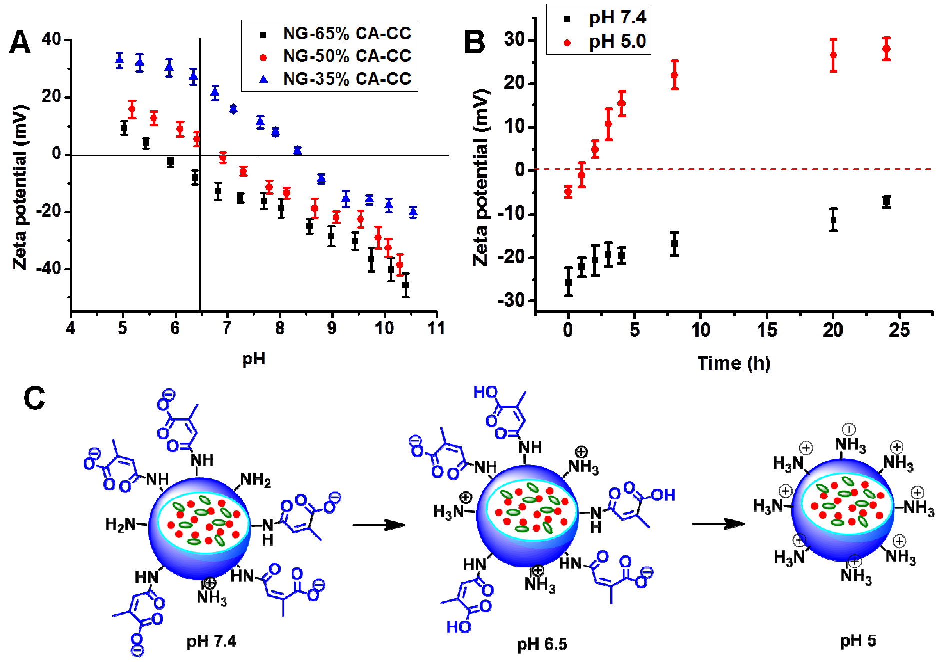

Figure 2. (A) The change of zeta potential for NGCA-CC with different CA functionalities over pH by pH titration; (B) the change of zeta potential for NGCA over time at pH 7.4 and 5.0; (C) schematic illustration of the two-stage charge conversion of zwitterionic nanogels.

3.3. Degradation of NGCA

The degradation behavior of NGCA was detected by DLS. In the presence of 5 mM ATP (Figure 3A), NGCA swelled after 1 h due to the partial cleavage of boronate ester crosslinkages caused by the competitive binding of ATP with boronic acid. After 24 h, NGCA was completely dissociated into precursors. As shown in Figure 3B, NGCA only swelled due to the partial cleavage of boronate ester at pH 5 after 24 h, which is in accordance with our previously published results.[29]

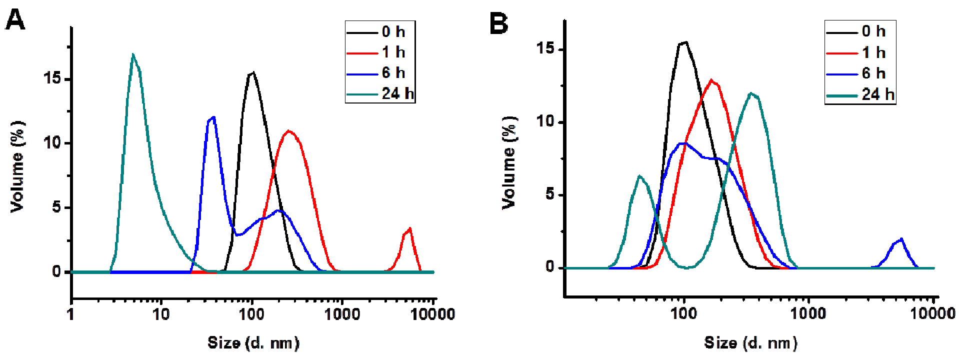

Figure 3. Degradation of NGCA determined over time with DLS (A) in the presence of 5 mM ATP at pH 7.4 and (B) at pH 5.

3.4. In vitro protein release

Figure 4 shows the release profiles of CC from NGCA-CC under different conditions. ATP and pH gradients between intracellular and extracellular environment are both important biological signals. At tumor extracellular pH (6.5), the release of CC was faster than that at pH 7.4. By lowering the pH, the electrostatic interaction between cationic CC and the anionic nanogel decreased because of the protonation of amino and carboxyl groups in the nanogel. When the pH decreased to 5, the boronate ester bond started to degrade, which induced the swelling of the nanogel and accelerated the CC release. In the intracellular ATP mimicking environment (5 mM ATP solution at pH 7.4), CC was released significantly faster compared to physiological conditions (pH 7.4). It has been reported that ATP can dissociate the boronate ester crosslinkers of the nanogel scaffold by competing with dPG.[29] The protein-loaded nanogels were prepared under mild conditions, which were not supposed to lead to protein denaturation or deactivation. CD analysis showed that the released CC possessed a similar profile to the native CC in the range from 200 to 240 nm (Figure S4), indicating that the secondary structure of CC was retained during encapsulation and release.

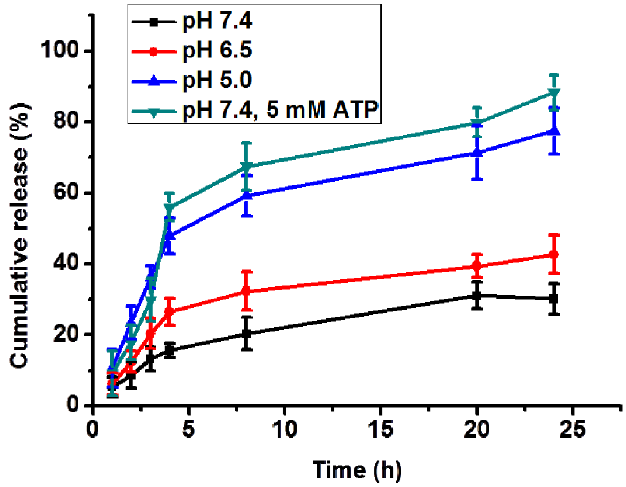

Figure 4. Release profiles of CC in buffer solutions with different pH or in the presence of 5 mM ATP.

3.5. In vitro cytotoxicity

The cytotoxicity of NGCA-CC and free CC were investigated by MTT assay (Figure 5A). Free CC caused a limited decrease in the cell viability and treatment with NGCA-CC induced a dose-dependent reduction of the cell viability. Since the MTT test did not show any obvious toxicity of NGCA towards MCF-7 cells up to a concentration of 1 mg/ml (Figure S5), the cell death was caused by the uptake and intracellular release of CC. A more detailed investigation about dose-dependent cytotoxicity was performed by RTCA (Figure S6), which presented consistent results with the MTT assay.

We further studied the influence of environmental pH on the antitumor activity of NGCA-CC. As shown in Figure 5B, NGCA-CC showed an obviously enhanced antitumor activity at pH 6.5 compared to that at pH 7.4. At pH 6.5, charge conversion rapidly occurred as discussed in Section 3.2 (Figure 2A) and produced positively charged NGCA-CC that should have exhibited a higher cellular uptake than the negative nanogel particles at pH 7.4. Free CC did not induce any toxicity on MCF-7 cells at both pH conditions. The RTCA analysis in Figure 5C also demonstrated a stronger inhibition of cell proliferation induced by NGCA-CC at pH 6.5 than pH 7.4.

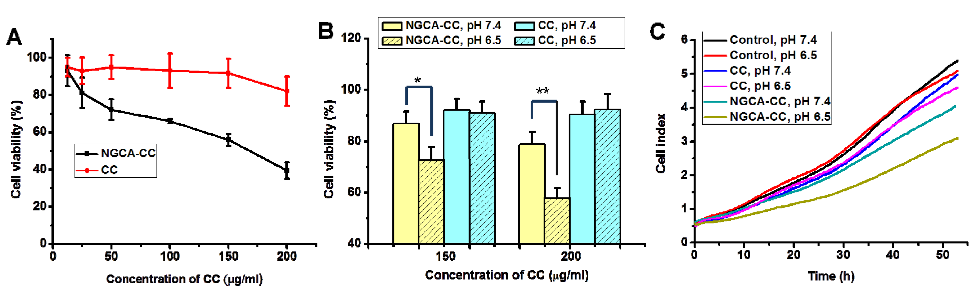

Figure 5. (A) In vitro cytotoxicity of NGCA-CC and free CC towards MCF-7 cells

determined by MTT assay at various CC concentrations for 48 h; in vitro cytotoxicity treated with substances at pH 7.4 or 6.5 for 1 h and further incubated in the fresh medium for 47 h by (B) MTT assay and (C) RTCA measurements. The untreated cells were set as a control. Data presented as the average ± standard deviation (Student's t-test, n = 4, *p < 0.05, **p < 0.01).

3.6. pH-dependent cellular uptake and intracellular protein release

In order to examine the influence of the charge conversional property on the tumor cellular uptake, MCF-7 cells were incubated respectively with NGCA-CC and free CC at pH 7.4 or 6.5 for 1 h. A red fluorescent endosome marker, FM 4-64, was used to stain the endosomes. CC was labeled with FITC according to the reported procedure.[40] As shown in Figure 6, the cellular uptake of NGCA-CC was higher at pH 6.5 than 7.4, demonstrating a pH-dependent uptake process of the nanogel. The enhanced cellular uptake at tumor extracellular condition (pH 6.5) was ascribed to the electrostatic absorption between the negatively charged cell membrane and the positively charged nanogels. In comparison, the uptake of free CC showed negligible change. In Figure S7, the quantitative internalization by flow cytometry was in accordance with the CLSM results. The charge conversion of NGCA-CC was an instantaneous process and a prompt response to pH change, unlike the relatively slower DMMA cleavage with its reaction time for the amide degradation.[16, 41]

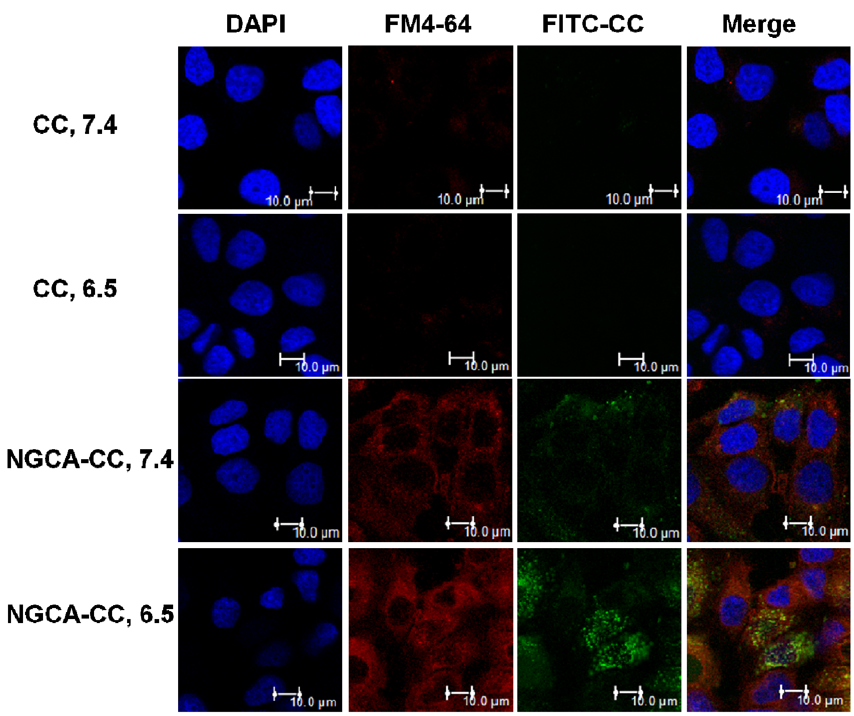

Figure 6. CLSM images of MCF-7 cells after the treatment of free CC or NGCA-CC, where CC is labeled with FITC, for 1 h at pH 7.4 or 6.5. The nuclei were stained with DAPI (blue) and the endosomes were stained with FM4-64 (red).

To determine whether or not the NGCA-CC could escape from the endosomal compartments, the cells were cultured in the substance-containing medium for 4 h and 24 h before measurement. In Figure 7, free CC showed negligible internalization at both time points. In comparison, a co-localization of NGCA-CC and endosomes, represented in yellow, was observed at 4 h. However, the green fluorescence of NGCA-CC showed an evident dissociation with the red fluorescence at 24 h (see enlarged images in Figure S8), which demonstrated their ability to endosomally escape. The probable reason is more amine groups can be exposed due to the cleavage of citraconic amide in the acidic endosomal environment, thus disrupting the endosomal membrane by the proton sponge effect.[42]

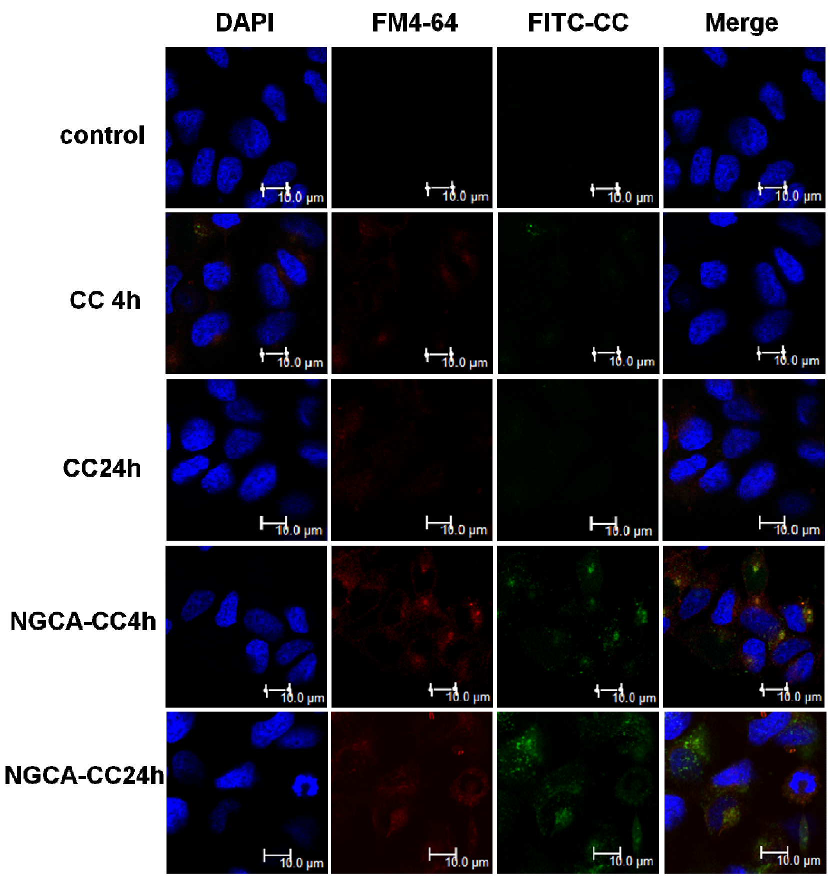

Figure 7. CLSM images of MCF-7 cells treated with free CC or NGCA-CC, in which CC was labeled with FITC, at 4 and 24 h. The nuclei were stained with DAPI (blue) and the endosomes were stained with FM4-64 (red).

3.7. Cell apoptosis

CC is a therapeutic protein that is able to induce programmed cell death by the mitochondria dependent apoptosis. The level of apoptosis was determined by annexin V-Alexa Fluor®488/PI staining using flow cytometry at a CC dosage of 50 μg/ml. NGCA did not induce higher cell apoptosis than the control even after 48 h treatment (Figure S9). Figure 8 shows the expression of annexin V and the permeation of PI in MCF-7 cells treated for 24 h with NGCA-CC and free CC, respectively. Quadrant 2

(Q2) showed the early apoptosis and quadrant 3 (Q3) represented the late apoptotic and necrotic cells. Only 13.8% (Q2+Q3) control cells exhibited apoptosis, whereas 27.8% apoptosis was induced by NGCA-CC. In contrast, much lower apoptosis was observed for free CC (18.5 %). Therefore, it is evident that the transfer of CC into cells was enhanced by the nanogel carriers so that it can more efficiently induce cell death by apoptosis.

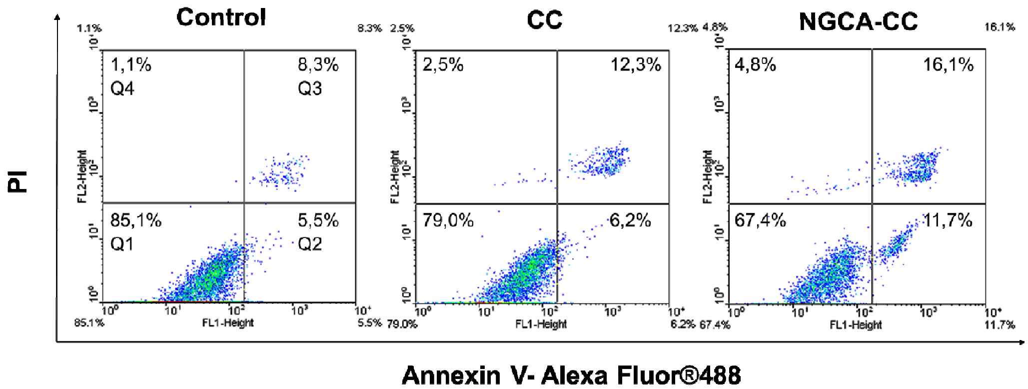

Figure 8. Contour diagram of Annexin V-Alexa Fluor®/PI flow cytometry of MCF-7 cells treated with free CC or NGCA-CC for 24 h with CC dosage of 50 µg/ml. ***Q1***: living cells. ***Q2*****:** early apoptotic cells. ***Q3*****:** late apoptotic and necrotic cells. ***Q4*****:** necrotic cells.

4. Conclusions

In conclusion, we designed and prepared a biodegradable zwitterionic nanogel with two-stage charge conversional properties for therapeutic protein delivery. The introduction of citraconic anhydride is, on the one hand, to provide carboxyl groups for complexing CC and offering the zwitterionic property for the first-stage charge conversion in the tumor extracellular environment, and, on the other hand, to form pH-cleavable citraconic amide that can release amino groups under the acidic organelle conditions for the second-stage charge conversion. Having escaped from the endosome, CC could be efficiently released due to the dissociation of nanogel in the ATP-containing cytosol, which resulted in cell death by mitochondria dependent apoptosis.

Acknowledgements

This study was supported by the Chinese Scholar Council (CSC), the focus area nanoscale of Freie Universität Berlin (www.nanoscale.fu-berlin.de), and the core-facility biosupramol (www.biosupramol.de). We thank Dr. Pamela Winchester for proofreading this manuscript, Dr. Katharina Achazi for the help with biological tests, Dr. Hua Fan for the support in flow cytometry experiments, and Florian Paulus for dPG synthesis.

References

1. D. V. Goeddel, D. G. Kleid, F. Bolivar, H. L. Heyneker, D. G. Yansura, R. Crea, T. Hirose, A.

Kraszewski, K. Itakura and A. D. Riggs, *PNAS*, 1979, **76**, 106-110.
2. Y. Lu, W. Sun and Z. Gu, *J. Control. Release*, 2014, **194**, 1-19.
3. D. Schrama, R. A. Reisfeld and J. C. Becker, *Nat. Rev. Drug Discov.*, 2006, **5**, 147-159.
4. T. Nochi, Y. Yuki, H. Takahashi, S.-i. Sawada, M. Mejima, T. Kohda, N. Harada, I. G. Kong, A. Sato, N. Kataoka, D. Tokuhara, S. Kurokawa, Y. Takahashi, H. Tsukada, S. Kozaki, K. Akiyoshi and H. Kiyono, *Nat. Mater.*, 2010, **9**, 572-578.
5. K. Y. Lee and S. H. Yuk, *Prog. Polym. Sci.*, 2007, **32**, 669-697.
6. Y. Lee, T. Ishii, H. Cabral, H. J. Kim, J.-H. Seo, N. Nishiyama, H. Oshima, K. Osada and K. Kataoka, *Angew. Chem. Int. Ed.*, 2009, **121**, 5413-5416.
7. X. Hu, J. Hu, J. Tian, Z. Ge, G. Zhang, K. Luo and S. Liu, *J. Am. Chem. Soc.*, 2013, **135**, 17617-17629.
8. E. C. Cho, J. Xie, P. A. Wurm and Y. Xia, *Nano Lett.*, 2009, **9**, 1080-1084.
9. S. E. A. Gratton, P. A. Ropp, P. D. Pohlhaus, J. C. Luft, V. J. Madden, M. E. Napier and J. M. DeSimone, *PNAS*, 2008, **105**, 11613-11618.
10. A. Muñoz Javier, O. Kreft, A. Piera Alberola, C. Kirchner, B. Zebli, A. S. Susha, E. Horn, S. Kempter, A. G. Skirtach, A. L. Rogach, J. Rädler, G. B. Sukhorukov, M. Benoit and W. J. Parak, *Small*, 2006, **2**, 394-400.
11. Z. Ge and S. Liu, *Chem. Soc. Rev.*, 2013, **42**, 7289-7325.
12. Y. Lee, S. Fukushima, Y. Bae, S. Hiki, T. Ishii and K. Kataoka, *J. Am. Chem. Soc.*, 2007, **129**, 5362-5363.
13. E. S. Lee, K. T. Oh, D. Kim, Y. S. Youn and Y. H. Bae, *J. Control. Release*, 2007, **123**, 19-26.
14. Z. Zhou, Y. Shen, J. Tang, M. Fan, E. A. Van Kirk, W. J. Murdoch and M. Radosz, *Adv. Funct. Mater.*, 2009, **19**, 3580-3589.
15. P. Xu, E. A. Van Kirk, Y. Zhan, W. J. Murdoch, M. Radosz and Y. Shen, *Angew. Chem. Int. Ed.*, 2007, **46**, 4999-5002.
16. J.-Z. Du, T.-M. Sun, W.-J. Song, J. Wu and J. Wang, *Angew. Chem. Int. Ed.*, 2010, **122**, 3703-3708.
17. J. Li, Y. Han, Q. Chen, H. Shi, S. ur Rehman, M. Siddiq, Z. Ge and S. Liu, *J. Mater. Chem. B*, 2014, **2**, 1813-1824.
18. W. Chen, K. Achazi, B. Schade and R. Haag, *J. Control. Release*, 2015, **205**, 15-24.
19. M. Meyer, A. Philipp, R. Oskuee, C. Schmidt and E. Wagner, *J. Am. Chem. Soc.*, 2008, **130**, 3272-3273.
20. J.-Z. Du, X.-J. Du, C.-Q. Mao and J. Wang, *J. Am. Chem. Soc.*, 2011, **133**, 17560-17563.
21. H. Tian, Z. Guo, L. Lin, Z. Jiao, J. Chen, S. Gao, X. Zhu and X. Chen, *J. Control. Release*, 2014, **174**, 117-125.
22. R. Mo, Q. Sun, J. Xue, N. Li, W. Li, C. Zhang and Q. Ping, *Adv. Mater.*, 2012, **24**, 3659-3665.
23. R. Mo, Q. Sun, N. Li and C. Zhang, *Biomaterials*, 2013, **34**, 2773-2786.
24. Y. Lee, T. Ishii, H. Cabral, H. J. Kim, J.-H. Seo, N. Nishiyama, H. Oshima, K. Osada and K. Kataoka, *Angew. Chem. Int. Ed.*, 2009, **48**, 5309-5312.
25. Y. Lee, T. Ishii, H. J. Kim, N. Nishiyama, Y. Hayakawa, K. Itaka and K. Kataoka, *Angew. Chem. Int. Ed.*, 2010, **49**, 2552-2555.
26. A. Sunder, R. Mülhaupt, R. Haag and H. Frey, *Adv. Mater.*, 2000, **12**, 235-239.
27. A. Sunder, R. Hanselmann, H. Frey and R. Mülhaupt, *Macromolecules*, 1999, **32**, 4240-4246.
28. S. Roller, H. Zhou and R. Haag, *Mol. Divers.*, 2005, **9**, 305-316.

29. X. Zhang, K. Achazi and R. Haag, *Adv. Healthc. Mater.*, 2015, **4**, 585-592.
30. M. Piest, M. Ankoné and J. F. J. Engbersen, *J. Control. Release*, 2013, **169**, 266-275.
31. X. Ma, L.-H. Zhang, L.-R. Wang, X. Xue, J.-H. Sun, Y. Wu, G. Zou, X. Wu, P. C. Wang, W. G. Wamer, J.-J. Yin, K. Zheng and X.-J. Liang, *ACS Nano*, 2012, **6**, 10486-10496.
32. A. B. Ryder, Y. Huang, H. Li, M. Zheng, X. Wang, C. W. Stratton, X. Xu and Y.-W. Tang, *J. Clin. Microbiol.*, 2010, **48**, 4129-4134.
33. J. M. Atienza, J. Zhu, X. Wang, X. Xu and Y. Abassi, *J. Biomol. Screen.*, 2005, **10**, 795-805.
34. K. Solly, X. Wang, X. Xu, B. Strulovici and W. Zheng, *ASSAY Drug Dev. Techn.*, 2004, **2**, 363-372.
35. J. Z. Xing, L. Zhu, J. A. Jackson, S. Gabos, X.-J. Sun, X.-b. Wang and X. Xu, *Chem. Res. Toxicol.*, 2005, **18**, 154-161.
36. X. Zhang, K. Achazi, D. Steinhilber, F. Kratz, J. Dernedde and R. Haag, *J. Control. Release*, 2014, **174**, 209-216.
37. D. Steinhilber, M. Witting, X. Zhang, M. Staegemann, F. Paulus, W. Friess, S. Küchler and R. Haag, *J. Control. Release*, 2013, **169**, 289-295.
38. E. K. Rofstad, B. Mathiesen, K. Kindem and K. Galappathi, *Cancer Res.*, 2006, **66**, 6699-6707.
39. X. Zhang, S. Malhotra, M. Molina and R. Haag, *Chem. Soc. Rev.*, 2015, **44**, 1948-1973.
40. I. I. Slowing, B. G. Trewyn and V. S. Y. Lin, *J. Am. Chem. Soc.*, 2007, **129**, 8845-8849.
41. X. Guo, C. Shi, G. Yang, J. Wang, Z. Cai and S. Zhou, *Chem. Mater.*, 2014, **26**, 4405-4418.
42. A. K. Varkouhi, M. Scholte, G. Storm and H. J. Haisma, *J. Control. Release*, 2011, **151**, 220-228.

A two-stage charge conversional nanogel with ATP/pH-sensitivity was generated by an inverse nanoprecipitation method. The first-stage charge conversion at tumor extracellular pH induced by the protonation of amine and carboxyl groups can enhance the tumor cellular uptake. In addition, the cleavage of citraconic amide in the acidic intracellular organelles (endo/lysosome) can induce the second-stage charge conversion due to the exposure of more amino groups that can disrupt the endosomal membrane, resulting in the endosomal escape.